

# Indolocarbazole-Based Ligands for Ladder-Type Four-Coordinate Boron Complexes

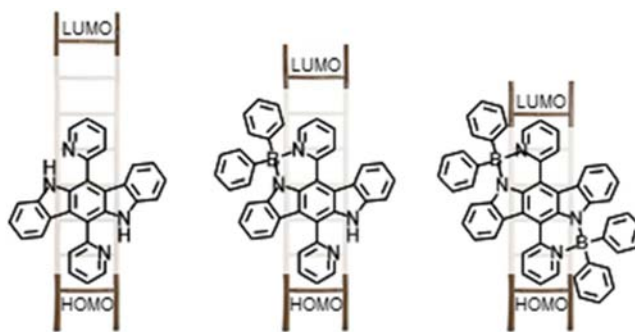
David Curiel,\* Miriam Más-Montoya, Laura Usea, Arturo Espinosa, Raúl A. Orenes, and Pedro Molina

Department of Organic Chemistry, Faculty of Chemistry, University of Murcia, Campus of Espinardo, Murcia 30100, Spain

davidcc@um.es

Received May 15, 2012

## ABSTRACT



A novel class of  $\pi$ -conjugated systems, which combine the indolo[3,2-*b*]carbazole unit with the formation of four-coordinate boron complexes, is presented. The resulting conjugated compounds have a double-laddered structure that provides interesting optical and electrochemical properties. The wide absorption range, covering most of the visible spectrum, along with the narrowing of the HOMO–LUMO energy gap, due to the presence of diphenylboryl centers, reinforces the potential of these molecules within the area of organic electronics.

Organoboron complexes have attracted much attention because of their outstanding optical properties. Regarding four-coordinate complexes, Bodipy derivatives are by far the most studied systems.<sup>1</sup> The versatility of the reported synthetic approaches has enabled a relatively easy adaptation of the Bodipy core which can be modified by attaching substituents to different positions (meso,  $\beta$ -pyrrolic, and boron center)<sup>2</sup> or by expanding the aromatic surface.<sup>3</sup> This

has resulted in compounds that can be tuned to absorb and/or emit over all the visible spectrum and even in the near-infrared.<sup>4</sup> Consequently, the different areas where these compounds have been applied cover a wide range of possibilities, such as molecular sensors,<sup>5</sup> fluorescent sensitizers,<sup>6</sup> imaging probes,<sup>7</sup> lasers,<sup>8</sup> electroluminescent devices,<sup>9</sup> or absorbing materials in organic solar cells.<sup>10</sup> This great potential has motivated the search for new  $\pi$ -conjugated ligands which can provide promising electronic and optical properties to the resulting four-coordinate

(1) (a) Benniston, A. C.; Copley, G. *Phys. Chem. Chem. Phys.* **2009**, *11*, 4124. (b) Ulrich, G.; Ziessel, R.; Harriman, A. *Angew. Chem., Int. Ed.* **2008**, *47*, 1184. (c) Loudet, A.; Burgess, K. *Chem. Rev.* **2007**, *107*, 4891.

(2) (a) Zhang, D.; Martin, V.; Garcia-Moreno, I.; Costela, A.; Perez-Ojeda, M. E.; Xiao, Y. *Phys. Chem. Chem. Phys.* **2011**, *13*, 13026. (b) Benniston, A. C.; Copley, G.; Lemmetyinen, H.; Tkachenko, N. V. *Eur. J. Org. Chem.* **2010**, 2867.

(3) (a) Zeng, L.; Jiao, C.; Huang, X.; Huang, K.-W.; Chin, W.-S.; Wu, J. *Org. Lett.* **2011**, *13*, 6026. (b) Tomimori, Y.; Okujima, T.; Yano, T.; Mori, S.; Ono, N.; Yamada, H.; Uno, H. *Tetrahedron* **2011**, *67*, 3187.

(4) (a) Ulrich, G.; Goeb, S. b.; De Nicola, A.; Retailleau, P.; Ziessel, R. *J. Org. Chem.* **2011**, *76*, 4489. (b) Ziessel, R.; Rihn, S.; Harriman, A. *Chem.—Eur. J.* **2010**, *16*, 11942. (c) Umezawa, K.; Matsui, A.; Nakamura, Y.; Citterio, D.; Suzuki, K. *Chem.—Eur. J.* **2009**, *15*, 1096.

(5) (a) Boens, N.; Leen, V.; Dehaen, W. *Chem. Soc. Rev.* **2012**, *41*, 1130. (b) Moragues, M. E.; Martinez-Manez, R.; Sancenon, F. *Chem. Soc. Rev.* **2011**, *40*, 2593.

(6) (a) He, H.; Si, L.; Zhong, Y.; Dubey, M. *Chem. Commun.* **2012**, 48, 1886. (b) Zhong, Y.; Si, L.; He, H.; Sykes, A. G. *Dalton Trans.* **2011**, 40, 11389.

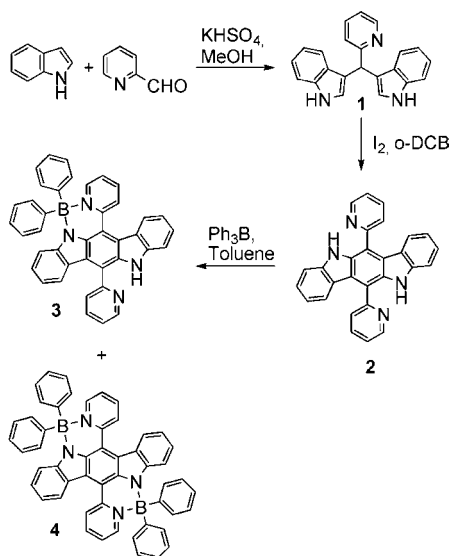
(7) (a) Kim, S.; Ohulchanskyy, T. Y.; Baev, A.; Prasad, P. N. *J. Mater. Chem.* **2009**, *19*, 3181. (b) Fan, J.; Guo, K.; Peng, X.; Du, J.; Wang, J.; Sun, S.; Li, H. *Sens. Actuators, B* **2009**, *142*, 191. (c) Domaille, D. W.; Zeng, L.; Chang, C. J. *J. Am. Chem. Soc.* **2010**, *132*, 1194.

(8) Perez-Ojeda, M. E.; Thivierge, C.; Martin, V.; Costela, A.; Burgess, K.; Garcia-Moreno, I. *Opt. Mater. Express* **2011**, *1*, 243.

boron complexes. In this regard, several N–N,<sup>11</sup> N–O,<sup>12</sup> N–C,<sup>13</sup> O–O,<sup>14</sup> or C–C<sup>15</sup> bidentate ligands have been reported in the literature. Since the fabrication of electronic devices requires the use of  $\pi$ -conjugated molecules that show good charge transport ability, the integration of boron complexes into ladder-type systems represents a useful strategy.<sup>16</sup> A very elegant approach consists in the rigidification of aromatic or heteroaromatic oligomers by virtue of boron coordination.<sup>17</sup> In our case, we present the integration of four-coordinate boron atoms into the structure of a ladder system such as indolo[3,2-*b*]carbazole, which has revealed itself as a good hole-transporting material in organic electronics.<sup>18</sup> Interestingly, the presence of boron centers will contribute to modify the electronic properties of the fused polyheteroaromatic unit.

The synthesis of the 6,12-disubstituted indolocarbazole was carried out in a three-step route (Scheme 1) that involved an initial condensation of pyridine-2-carboxaldehyde with indole to yield the corresponding 3,3'-(indolyl)methane, **1**.<sup>19</sup> This compound, when heated in the presence of iodine, has been proposed to evolve through a 3-arylideneindole, which dimerizes to yield 6,12-diarylidolo[3,2-*b*]carbazole, **2**.<sup>20</sup> The reaction of **2** with triphenylborane led to the isolation of two four-coordinate boron complexes, namely the mononuclear (9%), **3**, and the dinuclear (5%), **4**, compounds.

**Scheme 1.** Synthetic Route for the Ligand and Boron Complexes



All of the products were fully characterized by NMR spectroscopy (<sup>1</sup>H, <sup>13</sup>C, and <sup>11</sup>B) and mass spectrometry. Additionally, single crystals suitable for X-ray diffraction

(9) Yuan, W. Z.; Chen, S.; Lam, J. W. Y.; Deng, C.; Lu, P.; Sung, H. H. Y.; Williams, I. D.; Kwok, H. S.; Zhang, Y.; Tang, B. Z. *Chem. Commun.* **2011**, 47, 11216.

(10) (a) Yen, Y.-S.; Chou, H.-H.; Chen, Y.-C.; Hsu, C.-Y.; Lin, J. T. *J. Mater. Chem.* **2012**, 22, 8734. (b) Rousseau, T.; Cravino, A.; Ripaud, E.; Leriche, P.; Rihn, S.; De Nicola, A.; Ziessel, R.; Roncali, J. *Chem. Commun.* **2010**, 46, 5082. (c) Kumaresan, D.; Thummel, R. P.; Bura, T.; Ulrich, G.; Ziessel, R. *Chem.—Eur. J.* **2009**, 15, 6335.

analysis could be grown for the mononuclear complex **3** (Figure 1). It is worth highlighting the distortion of the indolocarbazole planarity as a result of the crystal packing and the structural stretching introduced by the chelation of the boron atom. The concave arrangement of the fused heteroaromatic system defines a 157.7° angle between the planes corresponding to each of the outer benzene rings. The pyridyl substituents are twisted out of the hypothetical plane containing the aromatic core. In addition, the boron atom forms a six-membered ring with a twisted-boat conformation. Different B–N bond lengths are observed for the pyridine (1.65 Å) and the indolocarbazole (1.54 Å) as a result of their dative and covalent nature, respectively. Conversely, B–C distances are almost identical (1.62 Å) for each phenyl ring. Despite the presence of some crystallization solvent molecules and the bulky diphenylboryl group, some intermolecular contacts are observed in the crystal packing. In this regard, molecules stack along the *a* axis following an ABC columnar pattern in which intra- and intercolumnar van der Waals interactions are detected between different indolocarbazole units (see the Supporting Information)

The thermal stability of both **3** and **4** was checked by thermogravimetric analysis (see the Supporting Information). Regarding the mononuclear complex **3**, an initial weight loss was detected slightly over 100 °C, presumably due to the release of solvent molecules trapped in the solid. After this, a decomposition curve was registered that showed a 5% weight loss at 400 °C. Similarly, compound **4** displayed a thermal profile whose decomposition temperature was 380 °C.

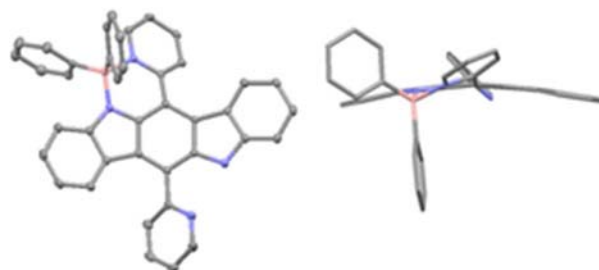


**Figure 1.** Two views of the crystal structure of compound **3**. Hydrogen atoms and crystallization solvent have been removed for the sake of clarity.

(11) (a) Araneda, J. F.; Piers, W. E.; Heyne, B.; Parvez, M.; McDonald, R. *Angew. Chem., Int. Ed.* **2011**, 50, 12214. (b) Kubota, Y.; Tsuzuki, T.; Funabiki, K.; Ebihara, M.; Matsui, M. *Org. Lett.* **2010**, 12, 4010. (c) Liu, Q.-D.; Mudadu, M. S.; Thummel, R.; Tao, Y.; Wang, S. *Adv. Funct. Mater.* **2005**, 15, 143.

(12) (a) Kubota, Y.; Hara, H.; Tanaka, S.; Funabiki, K.; Matsui, M. *Org. Lett.* **2011**, 13, 6544. (b) Frath, D.; Azizi, S. b.; Ulrich, G.; Retailleau, P.; Ziessel, R. *Org. Lett.* **2011**, 13, 3414. (c) Zhou, Y.; Xiao, Y.; Chi, S.; Qian, X. *Org. Lett.* **2008**, 10, 633.

(13) (a) Rao, Y.-L.; Amarné, H.; Wang, S. *Coord. Chem. Rev.* **2012**, 256, 759. (b) Yoshino, J.; Furuta, A.; Kambe, T.; Itoi, H.; Kano, N.; Kawashima, T.; Ito, Y.; Asashima, M. *Chem.—Eur. J.* **2010**, 16, 5026.

(14) (a) Nagai, A.; Kokado, K.; Nagata, Y.; Arita, M.; Chujo, Y. *J. Org. Chem.* **2008**, 73, 8605. (b) Ono, K.; Yoshikawa, K.; Tsuji, Y.; Yamaguchi, H.; Uozumi, R.; Tomura, M.; Taga, K.; Saito, K. *Tetrahedron* **2007**, 63, 9354.

(15) Zhao, Q.; Zhang, H.; Wakamiya, A.; Yamaguchi, S. *Synthesis* **2009**, 127.

Absorption spectra of the ligand **2** and the two complexes **3** and **4** were recorded in several solvents. In all cases, four well-resolved absorption bands were detected (Figure 2). According to the aromatic structure of the compounds, these bands could be ascribed to different  $\pi-\pi^*$  electronic transitions. In general, all three compounds displayed a hypsochromic effect upon increasing solvent polarity which, according to the Bayliss–McRae model, is interpreted as the ground state being more polar than the excited state.<sup>21</sup> The complexation of boron causes a gradual red shift of the absorption spectra on going from the plain indolocarbazole ligand, **2**, to the dinuclear complex **4** which is evident to the naked eye since the color of the complexes changes from yellow, **2**, to red, **3**, to dark green, **4**. In agreement with this result, a narrowing of the HOMO–LUMO gap (2.48, 2.05, and 1.76 eV for **2**, **3**, and **4** respectively) could be determined from the absorption spectra onset.

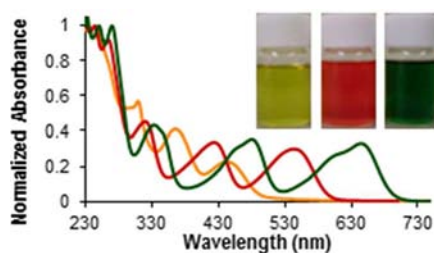


**Figure 2.** Absorption spectra of compounds **2** (yellow), **3** (red), and **4** (green) in  $\text{CH}_2\text{Cl}_2$  ( $2 \cdot 10^{-5}$  M).

The emission spectra recorded for **2**, **3**, and **4** displayed very weak fluorescence (see the Supporting Information). Although the emission efficiency increased upon boron chelation, the quantum yields of the complexes remained very low (Table 1). The general solvent effect shows again a hypsochromic shift. As previously discussed, the decrease in the HOMO–LUMO gap ( $\mathbf{2} > \mathbf{3} > \mathbf{4}$ ) also becomes evident in the significant red shift of the emission spectra.

The electrochemical properties were studied by cyclic voltammetry. All of the compounds **2–4** displayed two oxidation waves typical of the indolo[3,2-*b*]carbazole system (Figure 3). Interestingly, the coordination of the diphenylboryl group slightly widens the difference between the electrochemical processes by decreasing the potential for the first oxidation and increasing the potential for the second one. Moreover, the reversibility of the oxidation processes is enhanced by the presence of the chelated boron

atom, which is interpreted as an evidence of the higher stability of the intermediate radical cations.

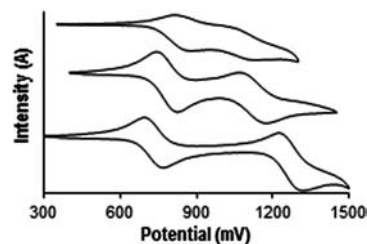


**Figure 3.** Cyclic voltammetry of compounds **2–4** in  $\text{CH}_2\text{Cl}_2$  ( $10^{-3}$  M) at room temperature,  $\text{TBAPF}_6$  (0.1 M), scan speed: 0.1 V/s, Ag/AgCl reference electrode, Pt working electrode.

The energy of the HOMOs can be estimated from the onset of the first oxidation wave.<sup>22</sup> The subtle differences, detected on the first oxidation potential, have a negligible influence on the HOMO energy. Thus, the presence of boron does not affect the ionization potential of the indolocarbazole system. Consequently, the gradual decrease in the HOMO–LUMO gap upon boron chelation results in an electronic structure of compounds **3** and **4**, where LUMOs are stabilized. The energy of these orbitals can be indirectly determined by adding the HOMO energy to the HOMO–LUMO optical gap (Table 1).

The significant stabilization of the LUMO results in one of the lowest values reported for a noncopolymeric indolo[3,2-*b*]carbazole derivative. In this regard, the HOMO and LUMO energies determined for compound **4** get close to the range of an ambipolar semiconductor which validates the strategy of boron chelation to modify the transporting properties of a heteroacenic semiconductor.<sup>23</sup>

**Table 1.** Optical and Electrochemical Characterization

	<b>2</b>	<b>3</b>	<b>4</b>
$\lambda_{\text{abs}}^a$ (nm)	441	545	643
$\epsilon$ ( $\text{M}^{-1} \text{cm}^{-1}$ )	8300	13375	19290
$\lambda_{\text{em}}$ (nm)	498	608	695
$\Phi^b$ (%)	0.4	6.4	2.8
$E_{1/2}^c$ (mV)	847; 1076	784; 1120	731; 1270
$E_{\text{onset}}$ (mV)	720	710	640
LUMO <sub>exp</sub> (eV)	−2.58	−3.00	−3.22
[LUMO <sub>theor</sub> ]	[−1.94]	[−2.40]	[−2.80]
HOMO <sub>exp</sub> (eV) <sup>d</sup>	−5.06	−5.05	−4.98
[HOMO <sub>theor</sub> ]	[−5.01]	[−5.01]	[−5.02]

(16) Agou, T.; Arai, H.; Kawashima, T. *Chem. Lett.* **2010**, *39*, 612.

(17) (a) Li, D.; Yuan, Y.; Bi, H.; Yao, D.; Zhao, X.; Tian, W.; Wang, Y.; Zhang, H. *Inorg. Chem.* **2011**, *50*, 4825. (b) Fukazawa, A.; Yamaguchi, E.; Ito, E.; Yamada, H.; Wang, J.; Irls, S.; Yamaguchi, S. *Organometallics* **2011**, *30*, 3870.

(18) (a) Boudreault, P.-L. T.; Virkar, A. A.; Bao, Z.; Leclerc, M. *Org. Electron.* **2010**, *11*, 1649. (b) Li, Y.; Wu, Y.; Gardner, S.; Ong, B. S. *Adv. Mater.* **2005**, *17*, 849.

(19) Deb, M. L.; Bhuyan, P. J. *Tetrahedron Lett.* **2006**, *47*, 1441.

(20) Deb, M. L.; Bhuyan, P. J. *Synlett* **2008**, 325.

(21) Bayliss, N. S.; McRae, E. G. *J. Phys. Chem.* **1954**, *58*, 1002.

<sup>a</sup> Recorded in dichloromethane ( $2 \times 10^{-5}$  M) at room temperature.

<sup>b</sup> Determined in ethanol at room temperature using anthracene as reference ( $\lambda_{\text{exc}(2)} = 410$  nm;  $\lambda_{\text{exc}(3)} = 480$  nm;  $\lambda_{\text{exc}(4)} = 500$  nm).

<sup>c</sup> Calculated from the anodic and cathodic peaks in cyclic voltammetry ( $E_{\text{pa}} + E_{\text{pc}}/2$ ). <sup>d</sup> Calculated from  $E_{\text{HOMO}} = -(4.34 + E_{\text{ox onset}})$ .

(22) (a) Loutfy, R. O.; Loutfy, R. O. *Can. J. Chem.* **1976**, *54*, 1454. (b) Kulkarni, A. P.; Tonzola, C. J.; Babel, A.; Jenekhe, S. A. *Chem. Mater.* **2004**, *16*, 4556. (c) D'Andrade, B. W.; Datta, S.; Forrest, S. R.; Djurovich, P.; Polikarpov, E.; Thompson, M. E. *Org. Electron.* **2005**, *6*, 11.

Theoretical calculations were carried out to get a better understanding of the electronic structure of the boron complexes. It is worth highlighting that whereas the HOMO is predominantly distributed along the fused polyheteroaromatic system defined by the indolocarbazole unit, the LUMO spreads along the axis described by the attached pyridines (Figure 4). Thus, the location of HOMO and LUMO depicts a perpendicular arrangement which outlines the double ladder structure of these indolocarbazole derivatives. The theoretical values determined for the frontier orbital energies show an excellent agreement for the HOMO and an approximately regular deviation for the LUMO when compared to the experimental values.

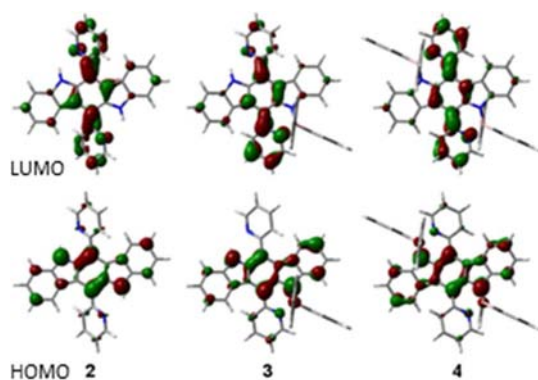


**Figure 4.** Computed Kohn–Sham isosurfaces (0.04 isovalue) for the frontier molecular orbitals.

Time-dependent DFT calculations were also performed for the interpretation of the UV–vis spectra (see the Supporting Information). According to these results, the lower energy bands for all three compounds are assigned to the  $S_0 \rightarrow S_1$  and  $S_0 \rightarrow S_2$  states which show a preferential correspondence with the HOMO  $\rightarrow$  LUMO and HOMO-1  $\rightarrow$  LUMO transitions, respectively. Higher energy bands involved contributions from several molecular orbitals. Regarding the distribution of molecular orbitals and the theoretical assignment of the absorption bands, the two lower energy bands denote a charge transfer identity. This could also be inferred from the larger solvatochromic effect detected for these two bands when compared to

(23) (a) Wang, C.; Dong, H.; Hu, W.; Liu, Y.; Zhu, D. *Chem. Rev.* **2012**, *112*, 2208. (b) Welch, G. C.; Coffing, R.; Peet, J.; Bazan, G. C. *J. Am. Chem. Soc.* **2009**, *131*, 10802.

(24) Reichardt, C.; Welton, T. *Solvents and Solvent Effects in Organic Chemistry*; John Wiley & Sons: New York, 2010.

higher energy bands within the same spectra, which are less solvent sensitive and would denote a more  $\pi \rightarrow \pi^*$  character.<sup>24</sup>

Considering the potential application of these boron complexes in the area of molecular electronics, absorption spectra were also registered for thin films prepared by spin coating from chloroform solutions (see the Supporting Information). A very good matching was detected between the solid-state spectra and those registered in solution, which means that the same energy levels are involved in the electronic transitions. As was also observed for the spectra registered in solution, when the thin film absorption spectra of **3** and **4** are superimposed, an alternation of the absorption maxima can be observed, resulting in a combined coverage which extends from the ultraviolet (200 nm) to the red region of the visible spectrum (750 nm). This feature might be interesting for the preparation of a dye blend for organic solar cells or even for tandem solar cells.<sup>25</sup>

To summarize, we have synthesized 6,12-di(pyridin-2-yl)indolo[3,2-*b*]carbazole as well as its mononuclear and dinuclear diphenylboranyl complexes. The electronic structure of these complexes has been determined by spectroscopic, electrochemical, and computational methods, revealing a narrowing effect of the HOMO–LUMO energy gap upon boron complexation. This narrowing is almost exclusively due to a decrease in the LUMO energy, which approaches the ambipolar materials energy range. The four-coordinate complexes show a wide absorption spectra which, when combined, cover most of the visible spectrum. These properties confer them the potential to be used in the area of organic electronics.

**Acknowledgment.** We are grateful to the Consejería de Universidades, Empresa e Investigación de la Región de Murcia, for financial support received through the Regional Plan of Science and Technology. We also acknowledge financial support from MICINN (project CTQ2008-01402 and M.M.-M. FPU fellowship).

**Supporting Information Available.** Experimental details, NMR spectra, thermogravimetric analysis, UV–vis spectra, fluorescence spectra, cyclic voltammetry, single-crystal X-ray diffraction data, and computational details. This material is available free of charge via the Internet at <http://pubs.acs.org>.

(25) (a) Ameri, T.; Dennler, G.; Lungenschmied, C.; Brabec, C. J. *Energy Environ. Sci.* **2009**, *2*, 347. (b) Rousseau, T.; Cravino, A.; Bura, T.; Ulrich, G.; Ziessel, R.; Roncali, J. *J. Mater. Chem.* **2009**, *19*, 2298.

The authors declare no competing financial interest.